



HAL
open science

Calibration of Digital Amateur Cameras

Magdalena Urbanek, Radu Horaud, Peter Sturm

► **To cite this version:**

Magdalena Urbanek, Radu Horaud, Peter Sturm. Calibration of Digital Amateur Cameras. [Research Report] RR-4214, INRIA. 2001. inria-00072405

HAL Id: inria-00072405

<https://inria.hal.science/inria-00072405>

Submitted on 24 May 2006

HAL is a multi-disciplinary open access archive for the deposit and dissemination of scientific research documents, whether they are published or not. The documents may come from teaching and research institutions in France or abroad, or from public or private research centers.

L'archive ouverte pluridisciplinaire **HAL**, est destinée au dépôt et à la diffusion de documents scientifiques de niveau recherche, publiés ou non, émanant des établissements d'enseignement et de recherche français ou étrangers, des laboratoires publics ou privés.

Calibration of Digital Amateur Cameras

Magdalena Urbanek — Radu Horaud — Peter Sturm

N° 4214

Juin 2001

THÈME 3



*Rapport
de recherche*

Calibration of Digital Amateur Cameras

Magdalena Urbanek , Radu Horaud , Peter Sturm

Thème 3 — Interaction homme-machine,
images, données, connaissances
Projet Movi

Rapport de recherche n° 4214 — Juin 2001 — 40 pages

Abstract: We introduce a novel outlook on the self-calibration task, by considering images taken by a camera in motion, allowing for zooming and focusing. Apart from the complex relationship between the lens control settings and the intrinsic camera parameters, a prior off-line calibration allows to neglect the setting of focus, and to fix the principal point and aspect ratio throughout distinct views. Thus, the calibration matrix is dependent only on the zoom position. Given a fully calibrated reference view, one has only one parameter to estimate for any other view of the same scene, in order to calibrate it and to be able to perform metric reconstructions. We provide a close-form solution, and validate the reliability of the algorithm with experiments on real images. An important advantage of our method is a reduced - to one - number of critical camera configurations, associated with it. Moreover, we propose a method for computing the epipolar geometry of two views, taken from different positions and with different (spatial) resolutions; the idea is to take an appropriate third view, that is "easy" to match with the other two.

Key-words: self-calibration, calibration, matching, 3D reconstruction, zoom.

Calibration de Caméras Numériques Amateurs

Résumé : Nous introduisons un nouveau regard sur l'auto-calibration, en considérant des images saisies par une caméra en mouvement, et soumises à des changements de la focale et de la mise au point. A priori, les relations entre ces paramètres et les paramètres internes du modèle sténopé sont complexes. Pourtant, nous montrons qu'en pratique, une pré-calibration permet le plus souvent de négliger les effets de la mise au point et de fixer le point principal et le rapport d'échelle pour des vues différentes. Ainsi la matrice de calibration ne dépend plus que de la distance focale. Etant donné une vue de référence calibrée, il suffit d'estimer un seul paramètre associé à une vue différente de la même scène pour la calibrer et faire des reconstructions métriques. Nous proposons une solution explicite et validons la fiabilité de l'algorithme en l'expérimentant sur des images réelles. Un avantage important de notre méthode est de réduire à un le nombre des mouvements critiques de la caméra. Aussi, nous proposons une méthode pour calculer la géométrie épipolaire de deux vues, prises sous des angles différents et des résolutions spatiales distinctes ; l'idée est de prendre une troisième vue appropriée, telle que l'appariement avec les deux autres soit aisé.

Mots-clés : auto-calibration, calibration, appariement d'images, reconstruction 3D, zoom.

Table of Contents

| | | |
|----------|---|-----------|
| 1 | Introduction | 5 |
| 1.1 | Previous work | 5 |
| 1.2 | Motivation | 5 |
| 1.3 | Contribution | 6 |
| 1.4 | Paper organization | 6 |
| 1.5 | Notations | 7 |
| 2 | Camera modeling | 8 |
| 2.1 | The model | 8 |
| 2.2 | Off-the-shelf digital camera | 8 |
| 3 | Off-line stability study over calibration | 8 |
| 3.1 | A way to calibrate | 9 |
| 3.2 | Optical distortion | 9 |
| 3.3 | Experiments | 9 |
| 3.4 | Dependencies | 11 |
| 3.5 | Reliability statistics | 14 |
| 3.5.1 | Experimental data | 16 |
| 3.5.2 | Is the distribution of α, u_0, v_0 Gaussian? | 16 |
| 3.5.3 | Statistically estimated variations | 19 |
| 3.6 | Final results to be used in self-calibration | 20 |
| 3.7 | What about another digital camera? | 21 |
| 4 | Self-calibration | 21 |
| 4.1 | Kruppa's equations | 21 |
| 4.2 | Outline of the algorithm | 24 |
| 4.3 | Critical motions | 24 |
| 5 | Matching | 25 |
| 5.1 | Difficulties | 26 |
| 5.2 | Our method | 26 |
| 5.3 | Outline of the algorithm | 30 |
| 6 | Experiments | 30 |
| 6.1 | Image pairs | 30 |
| 6.2 | Sequence of images | 31 |
| 6.3 | Discussion | 31 |
| 7 | 3D reconstruction | 34 |
| 8 | Conclusion | 34 |

| | | |
|----------|---|-----------|
| A | Link between images of the absolute conic and the fundamental matrix | 38 |
| B | Affine transformation between two views taken from the same camera position but with different resolutions | 39 |

1 Introduction

The problem of recovering the Euclidean structure of a scene is strongly associated with the estimation of the camera internal parameters, i.e. calibration. When no calibration knowledge provided, one can reconstruct only a projective model of the scene [6, 11].

1.1 Previous work

The most basic solution to compute the internal parameters employs a calibration grid or planes, and performs an off-line calibration. However the restriction of keeping an identical camera state (including zooming and focusing) while shooting subsequent images can hardly be fulfilled in practice.

Another idea is to self-calibrate an entire sequence. Existing approaches follow several directions. One is to assume invariance of unknown intrinsic parameters throughout distinct views [13, 18, 1, 9], thus not to allow for zooming/focusing, which is quite a strong constraint. Given a stereo pair of an arbitrary scene, one cannot vary but *the magnification parameter* (we use that term, to avoid confusion of associating different meanings to *the focal length*, in vision and optics), while having the other ones known [8]. Other methods [3, 14] allow the retrieval of varying magnification parameter and fixed principal point. Furthermore, if provided with at least 9 views, it is possible to fix only one camera internal parameter and let the other ones vary [14, 12].

In reality, such a general calibration problem cannot be solved reliably. On the other hand, one can quite easily provide some prior information, which simplifies the task. Our approach belongs to such a group of techniques.

1.2 Motivation

All considered cases of self-calibration, which allow magnification parameter variation throughout distinct views, suffer from a significant number of critical camera configurations [17]. It is therefore much "safer" not to change the camera settings.

Let us combine one fully calibrated image (*the reference image*) with an uncalibrated one, taken from a different viewpoint. Then, one has only one magnification parameter to estimate. What about the other intrinsic parameters? The complex relationship between calibration and camera lens control settings [19] does not allow straight-forward simplifications.

To summarize, we are interested in the following issues:

- Are there any conditions that enable the use of a priori knowledge of the intrinsic parameters?
- Can one allow for zooming/focusing, while still maintain a small family of critical situations?
- What can be done with stereo pairs, if one camera/view is fully calibrated?

1.3 Contribution

We combine off-line and on-line methods in order to calibrate a digital camera with a zoom lens and auto-focus.

We introduce a novel outlook on the self-calibration problem, by reducing to one the number of intrinsic parameters to be estimated. We provide a close-form solution for the method. Also, one has to account for only a single family of critical camera configurations [17].

By studying the behaviour of the camera intrinsic parameters as a function of variable zoom and focus, we derive approximate values for the aspect ratio, the principal point, and the magnification parameter for the boundary zoom positions. We verify the reliability of any of the approximations with statistical tests. We identify a small influence of focus upon calibration, which becomes negligible for settings larger than 2.5m. We conclude, that once a camera is calibrated for a known zoom setting, one can re-use those values any time that zoom is set. Therefore, we recommend employing minimally or maximally zoomed-in images as the reference ones, since those zoom settings can be reliably reproduced.

Furthermore, we simplify the computation of the epipolar geometry for stereo images of different resolutions, omitting a direct matching between them. The problem of matching two images of different zoom and viewpoint is therefore decomposed into two simpler matching problems: a wide baseline matching with the same zoom [2], and matching images with different zoom, shot from the same viewpoint [5].

The proposed method of "combined calibration" estimates the intrinsic parameters with even 2%-accuracy, from real images, leading to a reliable Euclidean reconstruction.

1.4 Paper organization

Section 2 defines the camera model and discusses properties of off-the-shelf digital cameras. A study on dependencies of the camera lens control settings on the calibration issue is presented in **Section 3**. **Section 4** encloses our self-calibration algorithm, along with a study of its critical cases. Further, in **Section 5** the problem of matching images with different spatial resolutions is addressed. Experiments on self-calibration of real images are presented in **Section 6**, followed by examples of a successful reconstruction of a real scene (**Section 7**), and the final conclusion (**Section 8**).

1.5 Notations

We distinguish different elements of vector space with different fonts. Also, we try to keep denoting exact space-objects with the same letters, throughout the whole paper.

| | |
|---------------------------|--|
| P | camera projection matrix |
| F | fundamental matrix |
| K | calibration matrix |
| A | affine transformation matrix |
| R | camera rotation matrix |
| \mathbf{t} | camera translation vector |
| M | world point |
| \mathbf{m}, \mathbf{m}' | points on images |
| \mathbf{e}, \mathbf{e}' | epipoles |
| Ω | absolute conic |
| ω | image of the absolute conic (3×3 matrix) |
| \mathbf{e}_i | the i -th vector from the canonical basis |
| $[\mathbf{v}]_{\times}$ | antisymmetric matrix associated with vector \mathbf{v} |
| \sim | equality up to scale |
| \mathbf{B}^T | transpose of a matrix \mathbf{B} |
| \mathbf{B}^{-1} | inverse of a matrix \mathbf{B} |
| \mathbf{B}^{-T} | transposed inverse of a matrix \mathbf{B} |

2 Camera modeling

2.1 The model

We assume the perspective camera model with the projection matrix of the form:

$$\mathbf{P} = \mathbf{K} (\mathbf{R} \ \mathbf{t}) \quad (1)$$

where \mathbf{R} and \mathbf{t} represent the orientation and the position of the camera with respect to the world coordinate system, and \mathbf{K} is the calibration matrix:

$$\mathbf{K} = \begin{pmatrix} k\alpha & 0 & u_0 \\ 0 & \alpha & v_0 \\ 0 & 0 & 1 \end{pmatrix}$$

with the principal point (u_0, v_0) , the magnification parameter α and the aspect ratio k . We assume a zero-skew.

A scene point \mathbf{M} is projected onto the image onto a point \mathbf{m} via $\mathbf{m} = \mathbf{P}\mathbf{M}$.

2.2 Off-the-shelf digital camera

Most often one is provided with digital cameras, which allow mechanical setting of both zoom and focus. One can specify the area of interest (and thus, its depth on the image) and focus on chosen features within the area.

We have worked with the Olympus Camedia C-2500L digital camera. It provides both auto-focus and manual-focus with discretized values from 0.3m until 15m and ∞ to be set. The zoom, on the contrary, has a continuous range and a manual drive, which makes the reproducibility of different settings difficult (with notable exceptions for the minimal and the maximal zooms).

Each $(zoom, focus)$ setting corresponds to a physical configuration of lenses, inside the camera. Since their functional dependencies are complex, we cannot specify the exact camera state, which makes the estimation of camera internal parameters difficult. When using auto-focus, the only camera settings that we are able to reproduce (and to expect the same calibration results, for an arbitrary image, taken with the same settings) are: $(zoom, focus) = (zoom_{min}, \infty)$ and $(zoom, focus) = (zoom_{max}, \infty)$.

The question is how do the entries of the calibration matrix \mathbf{K} change with variations of zoom and focus. Experiments described in the following section suggest conditions, under which the internal camera calibration can be assumed invariant, for different $(zoom, focus)$ settings.

3 Off-line stability study over calibration

We study the stability of the camera internal parameters, under change in the camera mechanical settings, zoom and focus. We point out the parameters that do not vary much,

and can be assumed invariant. We find a small influence of focus on calibration, if the camera is far enough from the scene. Finally, we provide calibration knowledge for particular zoom settings, which is to be used a priori, in self-calibration.

3.1 A way to calibrate

We extract the calibration matrix K from the projection matrix P , estimated from correspondences between non-coplanar 3D points and their 2D images.

The form of $P = (\bar{P} \quad \mathbf{p})$ and (1) imply: $\bar{P} = KR$. Since

$$\bar{P}\bar{P}^T = \underbrace{KRR^T}_I K^T = KK^T$$

we can simply obtain K from the Cholesky decomposition of $\bar{P}\bar{P}^T$.

In order to estimate P , we run a non-linear algorithm, which minimizes the reprojection error

$$C = \sum_{i=1}^n (u_i - u_{mi})^2 + (v_i - v_{mi})^2 \quad (2)$$

of n image points (u_i, v_i) and reprojections (u_{mi}, v_{mi}) of the corresponding 3D points \mathbf{M}_i .

3.2 Optical distortion

Since imperfect camera lenses give rise to non-perspective image distortion, it is often necessary to optimize (2) using additional distortion parameters. In some cases, this extended projection model causes over-parameterization, resulting in instabilities in the estimation of all intrinsic parameters.

Based on the observation, that the bigger the zoom used, the less distortion is present in the image, we can point out experimentally a "critical" zoom, for which the *estimated* distortion coefficient does not decrease with the increase of zoom. Therefore, we omit the distortion parameters in the optimization, if a zoom is bigger than the "critical" one.

We only estimate the first term D_r of the radial distortion, which proved sufficient to provide reliable results. Overall, the employed calibration method is described in [4].

3.3 Experiments

We stepped the lens through the full range of its control parameters - zoom and focus - and performed a full camera calibration, at each step (images of a calibration grid were considered). To ensure the stability of calibration, we considered only images with a sufficiently large number of control points clearly visible on an image of the grid. (The focused-in object can be neither too close nor too far away from the camera.)

We used manual focusing. For each focus value, the zoom was examined in different positions within its range of continuity. For each (*zoom, focus*) setting, we made several

| Focus[m] | k [1] | α [pix] | u_0 [pix] | v_0 [pix] | D_r [1] |
|----------|---------|----------------|-------------|-------------|-----------|
| 1 | 0.9993 | 700 | 321 | 268 | -0.2393 |
| | 0.9991 | 698 | 321 | 267 | -0.2423 |
| | 0.9999 | 700 | 317 | 267 | -0.2363 |
| 1.2 | 0.9992 | 695 | 314 | 277 | -0.2598 |
| | 0.9996 | 702 | 320 | 269 | -0.2405 |
| | 0.9997 | 728 | 294 | 238 | -0.1468 |
| 1.5 | 0.9998 | 731 | 316 | 232 | -0.1574 |
| | 1.0007 | 710 | 325 | 269 | -0.2469 |
| | 0.9998 | 723 | 318 | 234 | -0.1601 |
| 2 | 1.0007 | 736 | 295 | 269 | -0.1523 |
| | 1.0002 | 699 | 319 | 274 | -0.2970 |
| 2.5 | 1.0001 | 722 | 318 | 268 | -0.2207 |

Table 1: Calibration results: the *minimal* zoom and varying focus.

| Focus[m] | k [1] | α [pix] | u_0 [pix] | v_0 [pix] | D_r [1] |
|----------|---------|----------------|-------------|-------------|-----------|
| 1 | 0.9996 | 921 | 316 | 268 | -0.0976 |
| | 0.9994 | 920 | 318 | 268 | -0.0945 |
| | 0.9992 | 918 | 319 | 269 | -0.1037 |
| 1.2 | 1.0010 | 1133 | 320 | 266 | 0.0445 |
| | 1.0009 | 1122 | 317 | 274 | 0.0075 |
| | 1.0008 | 1128 | 318 | 271 | 0.0218 |
| 1.5 | 1.0015 | 1384 | 310 | 297 | 0 |
| | 1.0005 | 1386 | 291 | 296 | 0.0294 |
| | 1.0013 | 1391 | 320 | 292 | 0 |
| 2 | 1.0020 | 1749 | 312 | 313 | 0 |
| | 1.0020 | 1740 | 311 | 310 | 0 |
| | 1.0013 | 1745 | 289 | 303 | 0 |
| 2.5 | 1.0030 | 1969 | 301 | 324 | 0.1470 |
| | 1.0008 | 1944 | 255 | 316 | 0.0306 |
| 3.5 | 1.0024 | 1959 | 314 | 356 | 0.0295 |
| | 1.0012 | 1965 | 290 | 336 | 0 |
| 5 | 1.0016 | 1999 | 301 | 344 | 0.0182 |

Table 2: Calibration results: the *maximal* zoom and varying focus.

images with slightly different orientations of the calibration grid. The distance camera-grid was kept identical to the value of the set focus.

We considered focus values between 1m and 5m. The images were of size 640×512 pixels. Some of the obtained estimations¹ of the internal camera parameters are listed - separately

¹An additional numerous data used in those experiments is described in Section 3.5.1.

| Focus [m] | Zoom | k [1] | α [pix] | u_0 [pix] | v_0 [pix] | D_r [1] |
|-----------|--------------|---------|----------------|-------------|-------------|-----------|
| 1.2 | $z_1 > \min$ | 0.9997 | 823 | 314 | 267 | -0.1615 |
| | | 0.9997 | 817 | 319 | 270 | -0.1765 |
| | | 0.9992 | 816 | 317 | 271 | -0.1907 |
| 1.5 | $z_2 > \min$ | 1.0006 | 928 | 318 | 272 | -0.1259 |
| | | 1.0008 | 959 | 312 | 251 | -0.0288 |
| | | 1.0010 | 931 | 317 | 274 | -0.1311 |
| 1.5 | $z_3 > z_2$ | 1.0011 | 1078 | 313 | 268 | 0.0014 |
| 2 | $z_4 > \min$ | 1.0003 | 1044 | 318 | 273 | -0.0678 |
| | | 1.0007 | 1047 | 317 | 267 | -0.0303 |
| | | 1.0006 | 1042 | 316 | 270 | -0.0629 |
| 2.5 | $z_5 > \min$ | 1.0001 | 838 | 312 | 270 | -0.1661 |
| | | 1.0005 | 833 | 323 | 278 | -0.1982 |
| 2.5 | $z_6 > z_5$ | 1.0004 | 1034 | 317 | 269 | -0.0090 |
| 2.5 | $z_7 > z_6$ | 1.0001 | 1233 | 316 | 276 | 0.0105 |
| | | 1.0002 | 1238 | 316 | 274 | 0.0641 |
| 3.5 | $z_8 > \min$ | 1.0005 | 997 | 314 | 270 | -0.0319 |
| 5 | $z_9 > \min$ | 1.0011 | 1307 | 316 | 300 | -0.0533 |
| | | 1.0013 | 1353 | 309 | 302 | 0.0765 |

Table 3: Calibration results: varying zoom and focus.

- for the minimal zoom (Table 1), for the maximal zoom (Table 2), for varying zoom (Table 3).

3.4 Dependencies

What information can be extracted from Tables 1, 2 and 3 ?

- **Aspect ratio (k).** It is close to unity. The equality $k = 1$ is valid for any $(zoom, focus)$ setting, with a relative error 0.3% (see Figure 1).
- **Magnification parameter (α).** For the minimal zoom, α stays constant relative to focusing. For the maximal zoom, the same is observed as soon as the distance camera-object is bigger than 2.5m (see Figure 2). Hence, for a chosen zoom, it is possible to represent the relevant α with a single value (e.g. its mean): $\alpha_{min} = 739$ (with 4%-relative error) for $(zoom, focus) = (zoom_{min}, focus \geq 0.3m)$, and $\alpha_{max} = 1946$ (with 2%-relative error) for $(zoom, focus) = (zoom_{max}, focus \geq 2.5m)$.
- **Principal point (u_0, v_0).** Overall, it concentrates near the image centre (see Figures 3(c) and 4(c)). Since in general, the exact position of the principal point does not have big impact upon the quality of reconstruction, it is possible to employ approximate values: $u_0 = 311$ (with 7%-relative error), $v_0 = 280$ (with 15%-relative error).

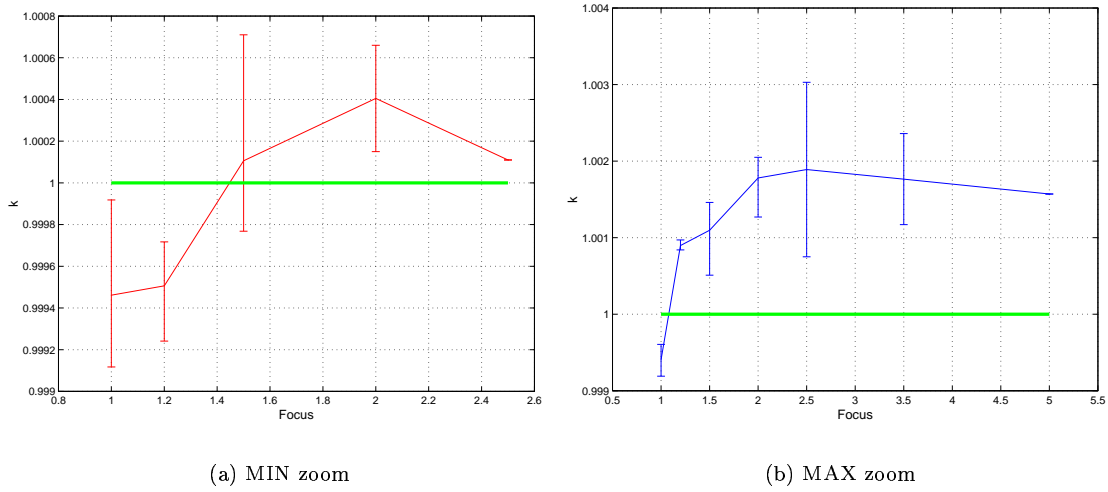


Figure 1: The aspect ratio k vs. focus: k keeps close to 1.

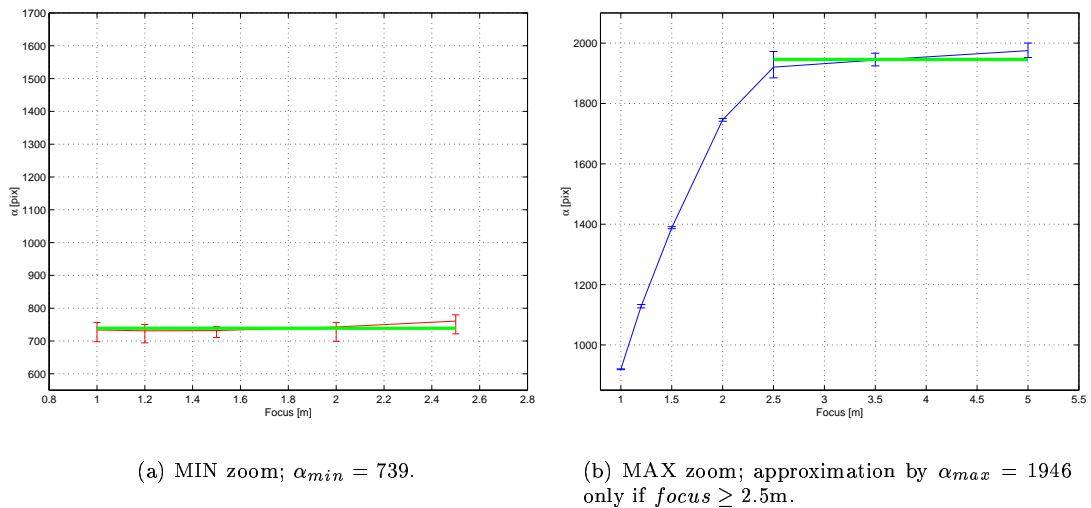
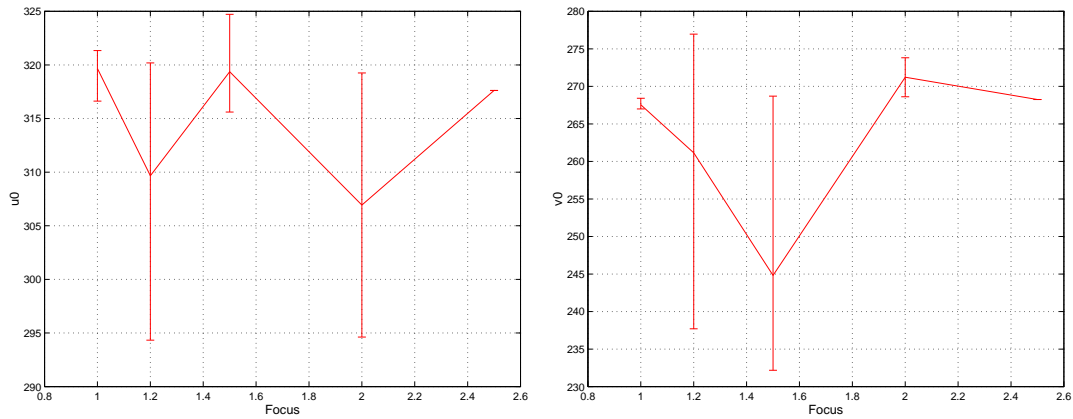
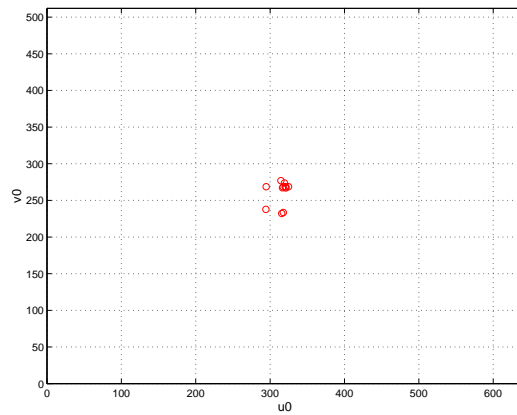


Figure 2: The magnification parameter α vs. focus: α can be approximated by its mean ($\alpha_{min}/\alpha_{max}$).



(a) Variations of u_0

(b) Variations of v_0



(c) (u_0, v_0)

Figure 3: The principal point (u_0, v_0) vs. focus - MIN zoom.

- **Auto-focusing.** For a fixed zoom, the setting of focus does not influence calibration significantly. We can use auto-focusing, and still be capable to employ calibration results for the examined zooms. We only have to keep in mind the requirement concerning the maximal zoom: the distance camera-scene has to be larger than 2.5m.

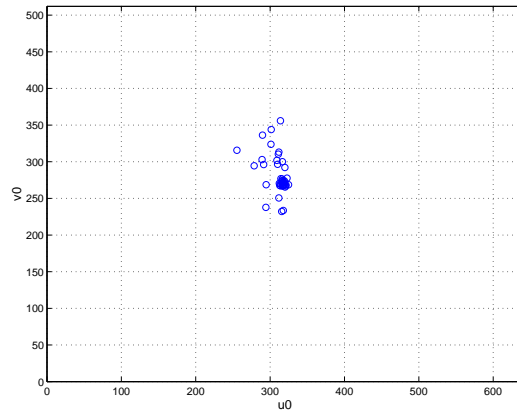
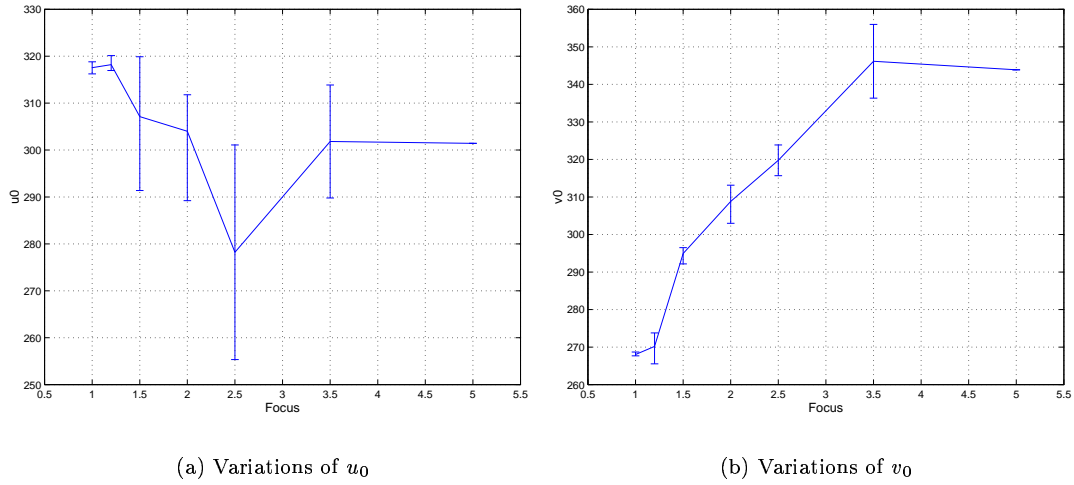


Figure 4: The principal point (u_0, v_0) vs. focus - MAX zoom.

3.5 Reliability statistics

We employed a statistical method to find out the risk of assuming invariance of some of the intrinsic camera parameters - $\alpha_{min}, \alpha_{max}, u_0, v_0$.

For a variable p (meaning anyone out of the intrinsic parameters), we aim to be able to represent it by a single value of its mean μ . An estimator \hat{p} of the mean μ has always some

uncertainty Δ . Therefore, our goal is to write:

$$p = \hat{p} \pm \Delta \quad \text{with a factor of risk } \gamma \quad (3)$$

which is equivalent to the likelihood of μ to belong to the area of uncertainty:

$$P(\mu \in [\hat{p} - \Delta, \hat{p} + \Delta]) = 1 - \gamma$$

In order to estimate \hat{p} and Δ , we use a method which requires knowledge of p distribution being Gaussian. As our data -each one of samples of $\alpha_{min}, \alpha_{max}, u_0, v_0$ - fulfills the constraint (we verify it later, in Section 3.5.2), we are able to apply the method, description of which follows. For more detailed studies over statistical properties and tests further employed, refer to [16] and [15].

Let us consider a sample of the variable p of elements $p^{(i)}, i = 1..N$, and let us assume that p follows the Gaussian distribution law with the mean μ and the standard deviation σ .

The experimental average is the best estimator of p . We use it as an approximation of μ , and denote it with \hat{p} :

$$\hat{p} = \frac{1}{N} \sum_{i=1}^N p^{(i)} \quad (4)$$

But, how close is μ to \hat{p} ?

We use the Student's t -statistic to measure the difference between the two means:

$$t = \frac{\hat{p} - \mu}{\hat{\sigma}}$$

where $\hat{\sigma}$ -assumed to be equal to σ^2 - is the experimental standard deviation:

$$\hat{\sigma} = \frac{1}{N(N-1)} \sum_{i=1}^N (p^{(i)} - \hat{p})^2$$

The fact that t follows the Student's distribution law with $N - 1$ degrees of freedom enables us to estimate the uncertainty Δ of the approximation of μ by \hat{p} . It is obtained by scaling $\hat{\sigma}$ with the Student's t -coefficient $t_{N,\gamma}$, defined for certain N and γ (γ being a factor of risk, also called *the significance level*):

$$\Delta = \hat{\sigma} \cdot t_{N,\gamma} \quad (5)$$

Altogether, in order to define a variable p in the way (3), one needs to employ equations (4) and (5).

²According to a sort of the Student's t -test, which measures the significance of a difference of means, when the two distributions are thought to have the same variance.

3.5.1 Experimental data

We took 48 images with the minimal zoom, and 48 images with the maximal zoom. We used auto-focusing in both cases. Focus was chosen arbitrary up to the constraint of being larger than 2.5 m, when dealing with the maximal zoom. We used the Olympus Camedia C-2500L digital camera.

We calibrated all of the 96 images, obtaining α, k, u_0, v_0 for each one of them.

Our tests concerned α, u_0 and v_0 (since k keeps very close to 1, thus can be assumed constant).

Tests for the magnification parameter α had to be made separately for different zooms, thus α_{min} and α_{max} . The principal point (u_0, v_0) , however, was treated altogether for any zoom chosen. Hence, we had 48-element samples to represent separately α_{min} and α_{max} , and 96-element-samples of u_0 and v_0 .

3.5.2 Is the distribution of α, u_0, v_0 Gaussian?

For a variable p (i.e. any of $\alpha_{min}, \alpha_{max}, u_0, v_0$), we verify the null hypothesis: " p follows the Gaussian distribution law with the mean μ (being the experimental mean of p) and the standard deviation σ (being the experimental standard deviation of p)".

Two kinds of tests were invoked:

- **Henry's line test** - makes use of a linear approximation of the inverse cumulative density function $icdf$ of the Gaussian distribution $N(\mu, \sigma)$ at point $p^{(i)}$:

$$W_i := icdf(\text{experimental probability } P(p \leq p^{(i)})) \approx \frac{p^{(i)} - \mu}{\sigma}$$

If p is of the Gaussian distribution, pairs $(p^{(i)}, W_i)$ are roughly aligned.

- **χ^2 test** - the hypothesis is accepted if: the difference between the experimental data distribution and the supposed distribution (represented by χ^2 decision statistic) is smaller than *level*, which is the inverse cumulative density function of the χ^2 -distribution of $N_B - 1$ degrees of freedom, with a risk γ . (N_B is the number of "bins", that data is sorted into; N_i is the number of events observed in the i th bin; n_i is the number expected according to the supposed distribution.)

$$\chi^2 = \sum_{i=1}^{N_B} \frac{(N_i - n_i)^2}{n_i} < (?) \text{ level}$$

Also, it is possible to visually verify the hypothesis, in an intuitive way, by the comparison between shapes of: the data histogram (based on the defined "bin"-division of the data range) and the hypothesized distribution's density function.

Decision statistic verification. For each parameter, its data sample was divided into such intervals ("bins"), that none of them were empty, and $N_i \geq 3$.

We supposed an equal factor of risk $\gamma = 0.05$ for every examined variable. The decision statistic χ^2 was then compared with *level*, which is different for different number of bins. Results are presented in Table 4.

| <i>param</i> | N_B | <i>level</i> | χ^2 | $\chi^2 < \textit{level}$? |
|----------------|-------|--------------|----------|-----------------------------|
| α_{min} | 9 | 12.59 | 6.43 | YES |
| α_{max} | 13 | 18.31 | 11.13 | YES |
| u_0 | 9 | 12.59 | 11.20 | YES |
| v_0 | 10 | 14.07 | 6.90 | YES |

Table 4: Verification of χ^2 related to *level*.

Graphical verification. Obtained plots are presented on Figures 5, 6, 7 and 8. Henry's test is illustrated on the part (a), and χ^2 test on the part (b) of each figure. Each of the parts (b) enables a visual comparison between the data histogram and some Gaussian distribution density function, with the parameters (μ, σ) depending on the data sample $p^{(i)}$: $(\mu, \sigma) = (\hat{p}, \hat{\sigma})$. Bins are defined identically as for the χ^2 decision variable test.

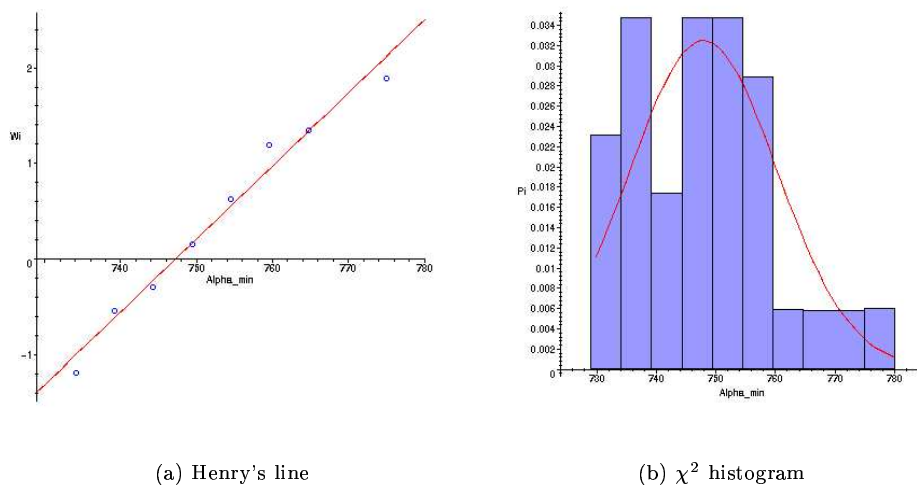
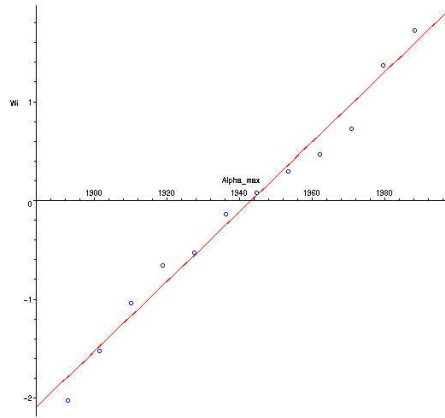
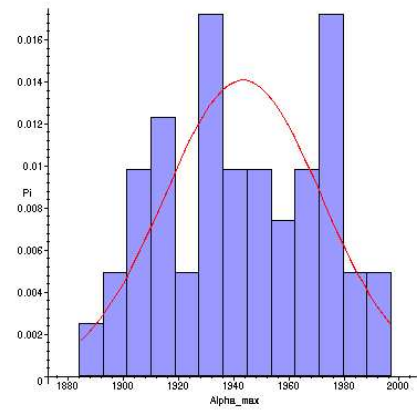


Figure 5: α_{min} - Gaussian distribution test

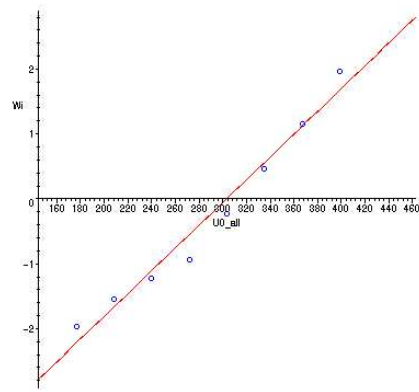


(a) Henry's line

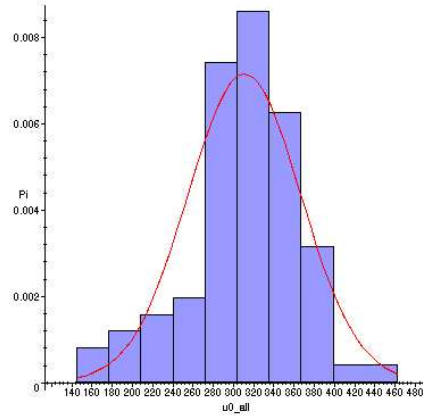


(b) χ^2 histogram

Figure 6: α_{max} - Gaussian distribution test

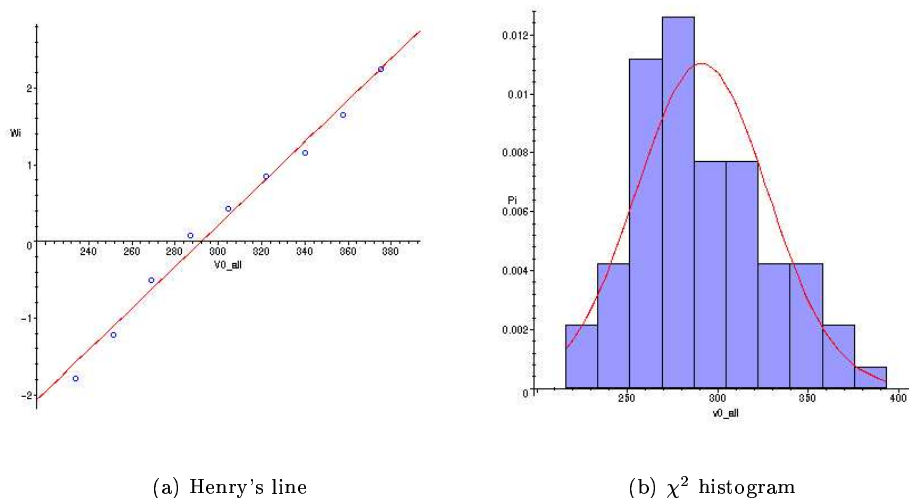


(a) Henry's line



(b) χ^2 histogram

Figure 7: u_0 - Gaussian distribution test



(a) Henry's line

(b) χ^2 histogram

Figure 8: v_0 - Gaussian distribution test

Interpretation. Parts (a) of Figures 5, 6, 7 and 8 present well aligned points, therefore -according to Henry's test- they vote for adequate internal parameters to follow the Gaussian distribution law. Similarly, parts (b) of the figures show histograms which shapes resemble quite well shapes of adequate Gaussian density functions.

More confirmation is obtained by examination of the decision variable χ^2 . Since in all cases it preserves the imposed constraint (see Table 4), one gets ensured that the distribution of each one of the examined internal parameters can be assumed Gaussian, with a possible 5%-error.

3.5.3 Statistically estimated variations

We have now the *right* to refer to (3) to describe statistically variations of $\alpha_{min}, \alpha_{max}, u_0, v_0$. When allowing the factor of risk $\gamma = 0.1$, we have:

$$\alpha_{min} = 739 \pm 34 \text{ (4.6\%)}$$

$$\alpha_{max} = 1946 \pm 47 \text{ (2.4\%)}$$

$$u_0 = 311 \pm 74 \text{ (23.9\%)}$$

$$v_0 = 280 \pm 55 \text{ (19.0\%)}$$

with relative variations given in parentheses.

The obtained results enable us to assume invariance of the camera intrinsic parameters, in specific cases. One can take advantage of that by using computed empirical mean values as a priori known estimations of adequate entries of the calibration matrix. Obviously, one cannot neglect the existence of errors. On the other hand, considered samples with numerous representative data encourage us to rely on the simplified estimations.

3.6 Final results to be used in self-calibration

A view taken with the minimal/maximal zooming. We are provided with calibration matrices of reference: K_{min} for the minimal zoom case (for any focus value), and K_{max} for the maximal zoom case (for focus ≥ 2.5 m).

A view taken with an arbitrary (unknown) zooming. One is provided with the values of k and (u_0, v_0) . Hence, α remains the only calibration parameter to determine.

A summary is given in Table 5.

| Zoom | Focus[m] | $k[1]$ | $\alpha[\text{pix}]$ | $u_0[\text{pix}]$ | $v_0[\text{pix}]$ |
|------------|------------|--------|----------------------|-------------------|-------------------|
| <i>min</i> | ≥ 0.3 | 1 | 739 | 311 | 280 |
| <i>max</i> | ≥ 2.5 | 1 | 1946 | 311 | 280 |
| ? | ? | 1 | ? | 311 | 280 |

Table 5: Results of off-line calibration (the Olympus Camedia C-2500L digital camera, images of the size 640×512 pixels).

Images of any size. For an image of the size $dim_u \times dim_v$ pixels, the calibration parameters have to be scaled by a factor λ , which is different for different parameters (see Table 6).

| <i>param</i> | k | α | u_0 | v_0 |
|--------------|---|---------------------|---------------------|---------------------|
| λ | $\frac{dim_u}{640} \cdot \frac{512}{dim_v}$ | $\frac{dim_u}{512}$ | $\frac{dim_u}{640}$ | $\frac{dim_v}{512}$ |

Table 6: Scale factor λ .

Then, each of the internal parameters -associated with an image of a *New Image Size*- can be obtained:

$$param_{NewImageSize} := \lambda \cdot param_{640 \times 512}$$

3.7 What about another digital camera?

We ran the off-line calibration process on another digital camera, Olympus Camedia C-1400L. The obtained estimations of the camera internal parameters (see Table 7) are according to the Student's reliability test, with a factor of risk 0.1 (refer to 3.5).

| Camera type | α [pix] | | k [1] | u_0 [pix] | v_0 [pix] |
|-------------------------|-----------------|-----------------|---------------|--------------|--------------|
| | <i>min zoom</i> | <i>max zoom</i> | | | |
| Olympus Camedia C-1400L | 878 ± 31 | 1896 ± 38 | 1 ± 0.003 | 265 ± 96 | 246 ± 37 |
| Olympus Camedia C-2500L | 739 ± 34 | 1946 ± 47 | 1 ± 0.003 | 311 ± 74 | 280 ± 55 |

Table 7: Off-line calibration of different cameras.

One can calibrate off-line any digital camera, obtaining values with divers reliability levels. Nevertheless, the process itself is correct, and results in estimations, which can be easily employed in further processes.

4 Self-calibration

We consider a stereo pair of images: a calibrated reference image and an image taken with an unknown zoom. (In practice, we obtain the calibration for the reference image simply by taking it using the minimal or the maximal zoom, and adopting the according intrinsic parameters, obtained by the off-line calibration.) We are thus provided with calibration matrices: K_{ref} , fully known, for the reference image, and K , defined up to unknown α , for the other image. Due to Kruppa's equations [10], we derive a close-form solution for α . Also, we reveal stereo configurations, for which our self-calibration algorithm fails.

4.1 Kruppa's equations

The idea is to take into account any internal calibration knowledge provided, does not matter whether it is full or partial.

One can separate already known entries of the calibration matrix K (k, u_0, v_0) from the unknown one (α):

$$K = \begin{pmatrix} k & 0 & u_0 \\ 0 & 1 & v_0 \\ 0 & 0 & 1 \end{pmatrix} \begin{pmatrix} \alpha & 0 & 0 \\ 0 & \alpha & 0 \\ 0 & 0 & 1 \end{pmatrix} = K_0 K_\alpha$$

and make K_0 denote the partial calibration knowledge.

On employing K_{ref} and K_0 , the epipolar constraint of the image pair, can be now put into a "semi-calibrated" space, obtaining \underline{E} :

$$\underline{E} = K_0^T F K_{ref} \quad (6)$$